Inhibition of thrombocyte activation restores protective immunity to mycobacterial infection

Elinor Hortle[1], Khelsey E. Johnson[2], Matt D. Johansen[1], Tuong Nguyen[1], Jordan A. Shavit[3], Warwick J. Britton[1,4], David M. Tobin[2], Stefan H. Oehlers[1,4] *

[1] Tuberculosis Research Program, Centenary Institute, Camperdown, NSW 2050, Australia

[2] Department of Molecular Genetics and Microbiology, Duke University School of Medicine, Durham, NC 27710, USA

[3] Department of Pediatrics and Cellular and Molecular Biology Program, University of Michigan, Ann Arbor, MI 48107, USA

[4] Central Clinical School and Marie Bashir Institute, The University of Sydney, Camperdown, NSW 2050, Australia

[*] Corresponding author email: s.oehlers@centenary.org.au, Twitter: @oehlerslab

Summary

Infection-induced thrombocytosis is a clinically important complication of tuberculosis infection. Recent studies have highlighted the utility of aspirin as a host-directed therapy modulating the inflammatory response to infection, but have not investigated the possibility of an anti-platelet mode of action. Here we utilise the zebrafish-*Mycobacterium marinum* model to show mycobacteria drive host haemostasis through the formation of granulomas. Treatment of infected zebrafish with aspirin markedly reduced mycobacterial burden. This effect is phenocopied by treatment with platelet-specific glycoprotein IIb/IIIa inhibitors demonstrating a detrimental role for infection-induced thrombocyte activation. We find that the reduction in mycobacterial burden is dependent on macrophages and granuloma formation providing the first *in vivo* experimental evidence that infection-induced platelet

activation compromises protective host immunity to mycobacterial infection. Our study illuminates platelet activation as an efficacious target of aspirin, a widely available and affordable host-directed therapy candidate for tuberculosis.

Keywords

Mycobacterial infection, haemostasis, innate immunity, clotting

Introduction

Mycobacterium tuberculosis is the world's most lethal pathogen, causing nearly 2 million deaths each year (World Health Organization. and Global Tuberculosis Programme.). The increasing incidence of both multi- and extremely- drug resistant tuberculosis (TB) urgently require the development of therapeutics that overcome the shortcomings of conventional antibiotics. Pathogenic mycobacteria co-opt numerous host pathways to establish persistent infection, and subversion of these interactions with host-directed therapies (HDTs) has been shown to reduce the severity of infection in animal models. For example, we have recently shown that mycobacteria induce host angiogenesis and increase host vascular permeability; blockade of either of these processes reduced both the growth and spread of bacteria (Oehlers et al., 2017; Oehlers et al., 2015). Therefore, host processes co-opted by the bacteria provide attractive targets for novel TB treatments. One such pathway may be haemostasis.

Thrombocytosis has long been recognised as a biomarker for advanced TB, and infection is often accompanied by the induction of a hyper-coagulable state, resulting in increased risk of deep vein thrombosis and stroke (Kutiyal et al., 2017; Robson et al., 1996). Recent evidence hints that mycobacteria may drive this process, and that it may aid their growth. For example, cell wall components from *M. tuberculosis* can induce expression of tissue factor - an

important activator of coagulation - in macrophages (Kothari et al., 2012). In mice and humans markers of platelet activation are upregulated during *M. tuberculosis* infection (Fox et al., 2018), and it has been shown *in vitro* that interaction with activated platelets increases the conversion of infected macrophages into cells permissive for bacterial growth (Feng et al., 2014; Fox et al., 2018). To date the pathogenic roles of haemostasis have not been studied in an intact *in vivo* model of mycobacterial infection.

Here we used the zebrafish-*M. marinum* model to investigate the role of host thrombocytes in mycobacterial infection. We show evidence that coagulation and thrombocyte activation are both bacterially driven, and that infection-induced activation of thrombocytes compromises protective immunity. However, clot formation itself has no effect on infection suggesting direct communication between the mycobacterial infection milieu and thrombocytes.

Results

Mycobacterium marinum induces coagulation in zebrafish.

To determine if *M. marinum* induces coagulation in zebrafish, we infected *Tg(fabp10a:fgb-EGFP)* transgenic embryos expressing EGFP tagged fibrinogen beta (FGB) with *M. marinum*-tdtomato, and imaged the developing infection every 15 minutes from 3 days post infection (DPI), until 6 DPI (Supplementary Video 1). We observed that clots formed only at areas of bacterial growth, and that the size of the clots increased as the number of bacteria increased over the course of the infection (Figure 1A). When we infected fish with ΔESX1 mutant *M. marinum* - which lacks the ability to export key virulence proteins, and does not

form granulomas – significantly less clot formation was observed (Figures 1B and 1C). Together, this data demonstrates that coagulation is a conserved consequence of infection driven by pathogenic mycobacteria across host species. Treatment with the anti-coagulant warfarin to prevent clot formation during infection (Figures 1D-E) did not affect bacterial burden, suggesting coagulation does not affect bacterial growth within the host (Figure 1F).

***Mycobacterium marinum* induces thrombosis in zebrafish.**

To determine if *M. marinum* induces thrombosis in zebrafish, we infected *Tg(cd41:GFP)* embryos, where thrombocytes are marked by GFP expression, with red fluorescent *M. marinum*. Infected embryos had significantly increased density of thrombocytes around the tail venous plexus where granulomas preferentially form (Figures S1A-B). Amongst infected embryos, there was a strong positive correlation between thrombocyte density and mycobacterial burden (Figure S1C). Both increased thrombocyte density, and a positive correlation between density and burden, were also observed in ΔESX1 mutant *M. marinum* infection (Figures S1C-D), suggesting that bacterially induced thrombosis is ESX1 independent.

Because the *cd41* promoter is active in non-motile thrombocyte precursors within their caudal haematopoietic tissue, we could not conclusively determine if these thrombocytes had actively migrated to and been retained at the site of infection (Lin et al., 2005). To determine if zebrafish thrombocytes are recruited to sites of mycobacterial infection, we performed trunk injection of *M. marinum* in *Tg(cd41:GFP)* at 3 days post fertilization (DPF), a time point after which mature thrombocytes are in the circulation. Embryos were then imaged at 2, 3, and 4 DPI. Thrombocytes were co-localised with sites of infection in 87% of fish. Rather than forming a stable and growing clot over a period of days (as we observed for FGB),

thrombocytes appeared to form transient associations with sites of infection (Figure S1D). In some instances, new thrombocytes seemed to be retained at sites of infection in different locations each day (Figure 2A I-IV), and in others, thrombocytes appeared to stay stationary for multiple days (Figure 2A V-VIII). The size of infection-associated thrombocytes varied greatly, suggesting activation and progressive degranulation or death of thrombocytes at sites of infection. Thrombocytes were most often observed on the edges of granulomas consistent with the location of granuloma-defining macrophages (Cronan et al., 2016).

Anti-platelet drugs reduce mycobacterial burden in zebrafish.

To determine if the previously reported infection-controlling effect of aspirin is conserved across vertebrate species (Mai et al., 2018), we treated *M. marinum*-infected fish with aspirin by immersion. Mycobacterial burden was reduced by approximately 50% in aspirin treated embryos (Figure 2A).

Although aspirin is a widely used platelet inhibitor, it is a broadly acting nonsteroidal anti-inflammatory drug that is known to modulate infection-relevant prostaglandin metabolism. Thus, to determine if the anti-platelet effects of aspirin treatment contribute to the reduced mycobacterial burden, we treated *M. marinum*-infected fish with the platelet-specific small molecule Glycoprotein IIb/IIIa inhibitor tirofiban or eptifibatide. Treatment with either Glycoprotein IIb/IIIa inhibitor phenocopied aspirin by reducing bacterial burden providing the first direct evidence of a detrimental role for platelet activation in the immune response to mycobacterial infection (Figure 2B-C).

Surprisingly, tirofiban treatment resulted in significantly higher number of visible thrombocytes at sites of infection compared to controls (Figures 2D-E). This suggests that, in contrast to our observations in the tail wound thrombosis model, tirofiban does not inhibit thrombocyte migration to areas of bacterial infection but may act by preventing activation and subsequent degranulation or death of zebrafish thrombocytes in response to mycobacterial infection.

We next examined the cellular target of anti-platelet drugs in our infection system. We performed antibacterial testing of the anti-platelet drugs in axenic cultures of *M. marinum* and did not observe any effect on bacterial growth *in vitro* demonstrating host-directed activity (Figure 2F).

The specificity of anti-platelet drugs against mycobacterial infection was tested in acute *Pseudomonas aeruginosa* infection. Treatment of *P. aeruginosa*-infected embryos with either class of anti-platelet drug did not affect survival demonstrating specificity against chronic mycobacterial infection (Figure 2G).

The anti-bacterial effect of anti-platelet drugs is thrombocyte dependent.

We next confirmed that anti-platelet drugs inhibit thrombocyte activation in zebrafish using a tail wound thrombosis assay (Figure S4A). Anti-platelet drugs reduced the number of thrombocytes recruited to tail wound clots demonstrating conservation of cellular target in zebrafish embryos (Figure S4B-C). Of the two Glycoprotein IIb/IIIa inhibitors tirofiban and eptifibatide, tirofiban is the more stable small molecule and therefore we chose to use tirofiban for inhibition of thrombocytes in all further experiments.

To determine if zebrafish thrombocytes are the conserved target for tirofiban in the zebrafish-*M. marinum* infection model, we inhibited thrombopoiesis by injection with a morpholino against the thrombopoietin receptor *cmpl* (Lin et al., 2005). Surprisingly, inhibition of thrombopoiesis did not affect the outcome of infection. However, tirofiban treatment failed to reduce bacterial burden in thrombocyte-depleted embryos, demonstrating thrombocytes are the cellular target of this drug in the zebrafish infection model (Figure 3A).

To confirm that tirofiban was acting specifically through inhibition of Glycoprotein IIb/IIIa, we performed infection experiments in Glycoprotein IIb/IIIa knock-out (KO) transgenic embryos (*itga2b* mutants). The *itga2b*^{sa10134} allele caused a dose-dependent reduction in thrombocytes recruited to tail wound clots (Figure S4A). As with *cmpl* knockdown, complete KO of *itga2b* had no effect on bacterial burden (Figure 3F), and thrombocyte accumulation at the site of infection was also unaffected (Figures S4B-C). However, heterozygous embryos phenocopied tirofiban treatment, showing a trend to reduced bacterial burden and increased thrombocyte accumulation (Figures 3B and S4B-C). This suggests that treatment with tirofiban may only partially inhibit Glycoprotein IIb/IIIa in our model.

Thrombocyte activation and coagulation are independently induced by mycobacterial infection.

We hypothesised that infection-induced coagulation and the resulting fibrin deposition in clots would activate thrombocytes through fibrin cross-linking. To investigate this hypothesis, we again used warfarin, which prevented clot formation during infection and did not affect bacterial burden (Figure 1E). Surprisingly, when warfarin was added to our tirofiban treatment model, it had no effect on the ability of tirofiban to reduce bacterial burden (Figure 3C).

To discount the possibility that warfarin and tirofiban co-treatment resulted in non-specific toxicity, we utilised a *fibrinogen alpha chain* mutant zebrafish line that does not readily form clots. Tirofiban treatment of FGA mutant zebrafish still significantly reduced bacterial burden further demonstrating that infection-induced activation of coagulation is not upstream of thrombocyte activation by mycobacterial infection (Figure 3D).

Conversely, we next asked if thrombocyte activation contributes to infection-induced coagulation. Analysis of FGB-GFP clots in tirofiban-treated embryos revealed reduced total clot formation (Figure 3E). However, correction for relative bacterial burden revealed that the reduced clot formation was a burden-dependent and thrombus formation was not additionally impacted by tirofiban treatment (Figure 3F).

Thrombocyte activation compromises immunity through granuloma-associated macrophages.

To further delineate the mechanism by which thrombocyte activation compromises innate immune control of mycobacterial infection but not the response to Pseudomonas infection, we asked if granuloma formation and maturation is essential to pathological thrombocyte activation.

To examine the requirement of granuloma formation and necrosis for thrombocyte-inhibiting drug efficacy, we infected embryos with ΔESX1 *M. marinum* that are unable to drive granuloma maturation or necrosis. Tirofiban treatment had no effect on mutant bacterial burden at 5 DPI (Figure 4A). Similarly, in embryos infected with *M. marinum* at a dose too low to form necrotic

granulomas by 5 DPI, continuous tirofiban treatment had no effect on bacterial burden at 5 DPI (Figure S6A).

We next took advantage of the stereotypical progression of innate immune granulomas in zebrafish embryos to investigate the temporal activity of thrombocyte inhibition by tirofiban. We found that at 3 DPI, a time-point with nascent granuloma formation but prior to significant granuloma organisation and necrosis, tirofiban had no effect on bacterial burden (Figure 4B). Conversely, treatment of infection from 4 to 5 DPI, a time-point when granulomas are organised and start to become necrotic, tirofiban significantly reduced bacterial burden within 24 hours (Figure 4C).

Macrophages are key cells in the innate granuloma, therefore to determine if thrombocyte inhibition exerts a protective effect through boosting macrophage-dependent immunity, we to depleted macrophages. We injected clodronate liposomes to deplete macrophages early during granuloma formation at 3 DPI (Figure S6B-C). Anti-platelet drug treatment was started immediately after liposome injection. In macrophage-depleted fish tirofiban did not reduce bacterial burden (Figure 4D).

It has previously been shown that in the presence of mycobacteria *in vitro*, platelets accelerate the conversion of macrophages to foam cells, which are permissive for mycobacterial growth, suggesting a mechanism for infection-induced thrombocytosis to compromise innate immunity to mycobacterial infection (Feng et al., 2014). We therefore hypothesised that thrombocyte inhibition would reduce the conversion of macrophages into foam cells. We investigated this by performing Oil-red O staining to measure lipid accumulation within individual granulomas (Figure 4E). Because tirofiban treatment reduced

bacterial burden, Oil-red O density was only compared between size-matched granulomas in treatment group. Tirofiban-treated embryos had significantly less Oil-red O accumulation in their granulomas when compared to DMSO control, even after correction for reduced bacterial burden (Figure 4F). Together, these data demonstrate an *in vivo* effect of thrombocyte activation inhibiting an effective immune response by converting macrophages into foam cells in mycobacterial granuloma.

Given that foam cell formation is closely associated with necrosis in tuberculosis (Russell et al., 2009) we hypothesised that tirofiban treatment would reduce cell death within the granuloma. We therefore used TUNEL staining to detect the fragmented DNA of dying cells in *M. marinum* infected embryos. At 5 DPI tirofiban-treated embryos showed significantly less TUNEL staining, indicating significantly reduced cell death within the granuloma (Figures 4G-H). Together these results suggest that infection-induced platelet activation aggravates a basal rate of macrophage cell death in the granuloma.

Discussion

Here we have used the zebrafish-*M. marinum* model to identify infection-induced haemostasis as a detrimental host response that is co-opted by pathogenic mycobacteria. Our data builds on previous studies that have shown coagulation, thrombocytosis and thrombocyte activation are associated with mycobacterial infection, and provide the first *in vivo* study to demonstrate a direct role for thrombocyte activation in promoting mycobacterial growth. We have shown that infection-induced haemostasis is conserved in the zebrafish-*M. marinum* infection model, and that the platelet inhibiting drugs aspirin, tirofiban, and

eptifibatide are able to reduce bacterial burden, independently of effects on coagulation, through host-mediated effects (Graphical abstract).

A number of studies have investigated aspirin as a possible adjunctive treatment for TB in both mice and humans (reviewed in (Hawn et al., 2013; Kalantri and Kalantri, 2018; Kroesen et al., 2017; Kroesen et al., 2018)). The results of these studies have been far from conclusive, with some finding beneficial effects, others finding no effect, and still others finding aspirin may reduce the effectiveness of anti-tubercular drugs. This lack of consensus may be due to the fact that NSAIDs affect many cell types and processes important for the host response to mycobacterial infection, not just coagulation and platelet activation. Our study expands this literature by demonstrating a significant reduction in bacterial burden following treatment with two specific anti-platelet drugs – tirofiban and eptifibatide, in addition to aspirin.

Our study found that coagulation and thrombocytes are independently activated by infection and have distinct roles during the pathogenesis of mycobacterial infection of zebrafish. Inhibiting coagulation alone did not significantly reduce bacterial burden, and therefore we considered anti-platelet treatment as a more attractive HDT than anti-coagulant treatment. Although we found lower total clot formation in tirofiban-treated embryos, this was only proportional to bacterial load suggesting infection-induced coagulation could be independent of infection-induced thrombocyte activation. It must be noted that we only measure a simple single end-point in our zebrafish embryo experiments (bacterial load) at a relatively early time point for a chronic infection. In more complex animals, where stroke and DVT are important secondary complications of mycobacterial infection, reducing coagulation may yet prove to be efficacious as a HDT to reduce morbidity. Conversely, data from the more complex mouse model of TB

suggests tissue factor-induced fibrin is necessary to contain mycobacteria within granulomas (Venkatasubramanian et al., 2016).

Our study provides evidence that infection-induced haemostasis is a conserved function of the core mycobacterial pathogenicity program centred around granuloma formation. Our experiments with ΔESX1 mutant *M. marinum*, which cannot secrete key virulence proteins that drive granuloma formation, demonstrated ESX1-dependent haemostasis and responsiveness to growth restriction by platelet inhibiting drugs. These data fit well with our observations that stationary thrombocytes were only observed around well-developed mycobacterial granulomas, and platelet inhibition was only effective at reducing bacterial burden after the development of significant granuloma pathology. Together these results point to a bidirectional relationship between thrombocyte activation and granuloma maturation (Figure 6).

Interestingly we observed that tirofiban treatment increased the number of thrombocytes accumulated at sites of infection. This may represent increased migration, increased accumulation through coagulation or decreased activation and subsequent degranulation/death. Given Tirofiban blocks the glycoprotein IIb/IIIa integrin - on which platelet migration is dependent (Gaertner et al., 2017) - and we observed that tirofiban reduced migration of thrombocytes in our tail wound model, we do not think that increased migration is likely. Similarly, an increase in coagulation ‘trapping’ thrombocytes at the site of infection is not supported by our experiments in *Tg(fabp10a:fgb-EGFP)* transgenic embryos. We therefore propose that this ‘increase’ actually represents a decrease in thrombocyte activation. Previous research has shown that during infection activated platelets can undergo phagocytosis and/or apoptosis (Feng et al., 2014; Gaertner et al., 2017; Hottz et al., 2014);

both of these processes would result in the loss of visible GFP+ thrombocytes from our system.

Recent research has highlighted the important role of platelets as innate immune cells; they are able to release anti-microbial peptides, pick up and 'bundle' bacteria, and initiate the recruitment of other innate immune cells to sites of infection (Gaertner et al., 2017; Li et al., 2017; Morrell et al., 2014). The low frequency at which direct thrombocyte-mycobacterial interactions were observed in our study argues against thrombocytes having a significant role in directly mediating immunity to mycobacterial infection. Our experiments demonstrating macrophage-dependence for anti-platelet drug mediated control of infection and reduced lipid accumulation in the granuloma, suggests infection-induced thrombocyte activation modulates macrophage containment of infection.

Our study joins several *in vitro* studies that have shown platelets can induce macrophages to have differential responses to bacteria or other pathologic stimuli. In the presence of *S. aureus*, thrombin activated platelets induce macrophages to increase phagocytosis and slow the growth of bacteria (Ali et al., 2017). Conversely, platelets can supress the macrophage response to LPS (Ando et al., 2016), and induce macrophages to produce less TNFa, more IL-10, and more IL-1ß in response to both BCG and *M. tuberculosis* (Feng et al., 2014; Fox et al., 2018). Crucially it has been shown that platelets are necessary for the formation of foam cells in the context of mycobacterial infection and atheroma (Feng et al., 2014). Our experiments with both Oil Red O and TUNEL demonstrate that thrombocytes induce similar pathways *in vivo* in response to *M. marinum*; directing macrophages towards foam-cell formation and necrosis.

Here we used the zebrafish-*M.marinum* model to show that mycobacteria drive coagulation and thrombosis through the formation of granulomas. We found that inhibition of thrombocyte activation was able to reduce foam-cell formation and cell death within the granuloma, leading to dramatically reduced bacterial burden. This is the first *in vivo* experimental evidence that infection-induced platelet activation contributes to the pathogenesis of mycobacterial infection. Our study identifies platelet activation as a potential target for tuberculosis host-directed therapy.

Acknowledgements

Dr Kristina Jahn and Sydney Cytometry for assistance with imaging equipment; Garvan Biological Testing Facility staff Ms Jennifer Brand, Mr Michael Pickering, Ms Rola Bazzi, Dr Lucie Nedved and Dr Stephanie Allison at the Garvan Institute of Medical Research for maintenance of zebrafish breeding stock; Professors Lalita Ramakrishnan, Shaun Jackson and Georges Grau, Associate Professor Carl Feng and Dr Jorn Coers for helpful discussion of results.

This work was supported by the Australian National Health and Medical Research Council APP1099912 and APP1053407; University of Sydney Fellowship; NSW Ministry of Health under the NSW Health Early-Mid Career Fellowships Scheme; and the Kenyon Family Inflammation Award (S.H.O.), Duke Summer Research Opportunities Program (K.J.), NIH Director's New Innovator Award 1DP2-OD008614 (D.M.T), NIH R01-HL124232 and R01-HL125774 (J.A.S.).

Author contributions

E.H., D.M.T. and S.H.O designed the experiments. E.H., K.E.J., M.D.J., T.N. and S.H.O performed the experiments. J.A.S. generated transgenic and mutant zebrafish lines. E.H. and S.O. wrote the paper. W.J.B., D.M.T. and S.H.O. supervised the project.

Declaration of Interests

The authors declare no competing interests.

References

Ali, R.A., Wuescher, L.M., Dona, K.R., and Worth, R.G. (2017). Platelets Mediate Host Defense against Staphylococcus aureus through Direct Bactericidal Activity and by Enhancing Macrophage Activities. J Immunol *198*, 344-351.

Ando, Y., Oku, T., and Tsuji, T. (2016). Platelets attenuate production of cytokines and nitric oxide by macrophages in response to bacterial endotoxin. Platelets *27*, 344-350.

Cronan, M.R., Beerman, R.W., Rosenberg, A.F., Saelens, J.W., Johnson, M.G., Oehlers, S.H., Sisk, D.M., Jurcic Smith, K.L., Medvitz, N.A., Miller, S.E., *et al.* (2016). Macrophage Epithelial Reprogramming Underlies Mycobacterial Granuloma Formation and Promotes Infection. Immunity *45*, 861-876.

Feng, Y., Dorhoi, A., Mollenkopf, H.J., Yin, H., Dong, Z., Mao, L., Zhou, J., Bi, A., Weber, S., Maertzdorf, J., *et al.* (2014). Platelets direct monocyte differentiation into epithelioid-like multinucleated giant foam cells with suppressive capacity upon mycobacterial stimulation. J Infect Dis *210*, 1700-1710.

Fox, K.A., Kirwan, D.E., Whittington, A.M., Krishnan, N., Robertson, B.D., Gilman, R.H., Lopez, J.W., Singh, S., Porter, J.C., and Friedland, J.S. (2018). Platelets Regulate Pulmonary Inflammation and Tissue Destruction in Tuberculosis. Am J Respir Crit Care Med.

Gaertner, F., Ahmad, Z., Rosenberger, G., Fan, S., Nicolai, L., Busch, B., Yavuz, G., Luckner, M., Ishikawa-Ankerhold, H., Hennel, R., *et al.* (2017). Migrating Platelets Are Mechano-scavengers that Collect and Bundle Bacteria. Cell *171*, 1368-1382 e1323.

Hawn, T.R., Matheson, A.I., Maley, S.N., and Vandal, O. (2013). Host-directed therapeutics for tuberculosis: can we harness the host? Microbiol Mol Biol Rev *77*, 608-627.

Hottz, E.D., Medeiros-de-Moraes, I.M., Vieira-de-Abreu, A., de Assis, E.F., Vals-de-Souza, R., Castro-Faria-Neto, H.C., Weyrich, A.S., Zimmerman, G.A., Bozza, F.A., and Bozza, P.T. (2014). Platelet activation and apoptosis modulate monocyte inflammatory responses in dengue. J Immunol *193*, 1864-1872.

Johansen, M.D., Kasparian, J.A., Hortle, E., Britton, W.J., Purdie, A.C., and Oehlers, S.H. (2018). Mycobacterium marinum infection drives foam cell differentiation in zebrafish infection models. bioRxiv.

Kalantri, A., and Kalantri, S. (2018). Can aspirin help? Elife *7*.

Kothari, H., Rao, L.V., Vankayalapati, R., and Pendurthi, U.R. (2012). Mycobacterium tuberculosis infection and tissue factor expression in macrophages. PLoS ONE *7*, e45700.

Kroesen, V.M., Groschel, M.I., Martinson, N., Zumla, A., Maeurer, M., van der Werf, T.S., and Vilaplana, C. (2017). Non-Steroidal Anti-inflammatory Drugs As Host-Directed Therapy for Tuberculosis: A Systematic Review. Front Immunol *8*, 772.

Kroesen, V.M., Rodriguez-Martinez, P., Garcia, E., Rosales, Y., Diaz, J., Martin-Cespedes, M., Tapia, G., Sarrias, M.R., Cardona, P.J., and Vilaplana, C. (2018). A Beneficial Effect of Low-Dose Aspirin in a Murine Model of Active Tuberculosis. Front Immunol *9*, 798.

Kutiyal, A.S., Gupta, N., Garg, S., and Hira, H.S. (2017). A Study of Haematological and Haemostasis Parameters and Hypercoagulable State in Tuberculosis Patients in Northern India and the Outcome with Anti-Tubercular Therapy. Journal of clinical and diagnostic research : JCDR *11*, OC09-OC13.

Li, J.L., Zarbock, A., and Hidalgo, A. (2017). Platelets as autonomous drones for hemostatic and immune surveillance. J Exp Med.

Lin, H.F., Traver, D., Zhu, H., Dooley, K., Paw, B.H., Zon, L.I., and Handin, R.I. (2005). Analysis of thrombocyte development in CD41-GFP transgenic zebrafish. Blood *106*, 3803-3810.

Mai, N.T., Dobbs, N., Phu, N.H., Colas, R.A., Thao, L.T., Thuong, N.T., Nghia, H.D., Hanh, N.H., Hang, N.T., Heemskerk, A.D., *et al.* (2018). A randomised double blind placebo controlled phase 2 trial of adjunctive aspirin for tuberculous meningitis in HIV-uninfected adults. eLife *7*.

Matty, M.A., Oehlers, S.H., and Tobin, D.M. (2016). Live Imaging of Host-Pathogen Interactions in Zebrafish Larvae. Methods Mol Biol *1451*, 207-223.

Morrell, C.N., Aggrey, A.A., Chapman, L.M., and Modjeski, K.L. (2014). Emerging roles for platelets as immune and inflammatory cells. Blood *123*, 2759-2767.

Oehlers, S.H., Cronan, M.R., Beerman, R.W., Johnson, M.G., Huang, J., Kontos, C.D., Stout, J.E., and Tobin, D.M. (2017). Infection-induced vascular permeability aids mycobacterial growth. J Infect Dis *215*, 813-817.

Oehlers, S.H., Cronan, M.R., Scott, N.R., Thomas, M.I., Okuda, K.S., Walton, E.M., Beerman, R.W., Crosier, P.S., and Tobin, D.M. (2015). Interception of host angiogenic signalling limits mycobacterial growth. Nature *517*, 612-615.

Passeri, M.J., Cinaroglu, A., Gao, C., and Sadler, K.C. (2009). Hepatic steatosis in response to acute alcohol exposure in zebrafish requires sterol regulatory element binding protein activation. Hepatology *49*, 443-452.

Robson, S.C., White, N.W., Aronson, I., Woollgar, R., Goodman, H., and Jacobs, P. (1996). Acute-phase response and the hypercoagulable state in pulmonary tuberculosis. Br J Haematol *93*, 943-949.

Russell, D.G., Cardona, P.J., Kim, M.J., Allain, S., and Altare, F. (2009). Foamy macrophages and the progression of the human tuberculosis granuloma. Nat Immunol *10*, 943-948.

Venkatasubramanian, S., Tripathi, D., Tucker, T., Paidipally, P., Cheekatla, S., Welch, E., Raghunath, A., Jeffers, A., Tvinnereim, A.R., Schechter, M.E., *et al.* (2016). Tissue factor expression by myeloid cells contributes to protective immune response against Mycobacterium tuberculosis infection. Eur J Immunol *46*, 464-479.

Vo, A.H., Swaroop, A., Liu, Y., Norris, Z.G., and Shavit, J.A. (2013). Loss of fibrinogen in zebrafish results in symptoms consistent with human hypofibrinogenemia. PLoS ONE *8*, e74682.

Walton, E.M., Cronan, M.R., Beerman, R.W., and Tobin, D.M. (2015). The Macrophage-Specific Promoter mfap4 Allows Live, Long-Term Analysis of Macrophage Behavior during Mycobacterial Infection in Zebrafish. PLoS ONE *10*, e0138949.

World Health Organization., and Global Tuberculosis Programme. Global tuberculosis control : WHO report. (Geneva, Global Tuberculosis Programme), p. 15 volumes.

Figure legends

Figure 1: *Mycobacterium marinum* induces coagulation and thrombosis around sites of infection in zebrafish

A) Representative images of a *Tg(fabp10a:fgb-EGFP)* embryo infected with *M.marinum*-tdTomato by caudal vein injection, showing clot formation (green) at sites of infection (red) at 3, 4, and 5 days post infection. B) Representative images of 5 DPI *Tg(fabp10a:fgb-EGFP)* embryos infected with *M.marinum*-tdTomato WT and ΔESX1 *M. marinum*-td-tomato (ΔESX1) showing clot formation (green) at sites of infection (red). Arrows indicate clotting. C) Quantification of clot formation in burden-matched ΔESX1 mutant-infected *Tg(fabp10a:fgb-EGFP)* embryos normalised to WT *M. marinum* control. Error lines represent mean ± SEM, statistical analysis by T test. Data show combined results from two independent experiments. D) Representative images of *Tg(fabp10a:fgb-EGFP)* embryos, where clot formation can be visualised by GFP fluorescence, infected with *M.marinum*-tdTomato (red) and treated with either DMSO or warfarin. E) Quantification of clotting in warfarin-treated *Tg(fabp10a:fgb-EGFP)* embryos. F) Quantification of bacterial burden in embryos treated with warfarin. Data are combined results of two independent experiments. F) Representative 2DPI, 3DPI and 4DPI images of *Tg(cd41:GFP)* fish infected with *M.marinum*-tdTomato at 3DPF. White arrow heads show thrombocyte (green) association with areas of bacterial growth (red). Thrombocytes not indicated with an arrow head were circulating and not considered to be associated with bacteria (more detail available in Figure S2C).

Figure 2: Anti-platelet drugs reduce bacterial burden in *M. marinum* infection

A) Quantification of bacterial burden in embryos treated with aspirin normalised to DMSO control. Data are combined results of two independent experiments. B) Quantification of bacterial burden in embryos treated with tirofiban normalised to DMSO control. Data are combined results of two independent experiments. C) Quantification of bacterial burden in embryos treated with eptifibatide or DMSO control. D) Representative images of

Tg(cd41:gfp) embryos treated with tirofiban or DMSO control. E) Quantification of total thrombocyte *Tg*(*cd41:GFP)* area within the tail of infected larvae treated with tirofiban. F) Quantification of bacterial growth by relative fluorescence in 7H9 broth culture supplemented with drugs as indicated. G) Survival analysis of *P. aerogenosa* PA01 infected embryos treated with anti-platelet drugs as indicated.

All graphs show Mean ± SEM. Statistical analyses performed by T tests and Log-Rank tests where appropriate.

Figure 3: The anti-bacterial effect of anti-platelet drugs is thrombocyte dependent

A) Total fluorescence area of *M. marinum* bacteria in larvae injected with either control or cmpl morpholino (MO) to deplete thrombocytes, and then treated with tirofiban (Tiro). Values are normalised to DMSO treated control MO larvae. Graphs show the combined results of 2 independent experiments. B) Quantification of bacterial burden in in *itga2b* mutant embryos normalised to WT control. Data are combined results of four independent experiments. C) Quantification of bacterial burden in embryos treated with tirofiban, warfarin, or tirofiban and warfarin, normalised to DMSO control. Data are combined results of two independent experiments. D) Quantification of bacterial burden in *fga*$^{-/-}$ embryos treated with tirofiban. E) Representative images of 5 DPI *Tg(fabp10a:fgb-EGFP)* embryos infected with *M.marinum*-tdTomato and treated with either DMSO or tirofiban. F) Quantification of clotting relative to bacterial burden in embryos treated with tirofiban normalised to DMSO control. Data are combined results of two independent experiments.

All graphs show Mean ± SEM. Statistical analyses performed by T tests or ANOVA where appropriate.

Figure 4: Thrombocyte activation compromises immunity through granuloma-associated macrophages.

A) Quantification of bacterial burden in embryos infected with ΔESX1 *M.marinum*-tdTomato and treated with tirofiban. B) Quantification of bacterial burden at 3 DPI after continuous tirofiban treatment from 0 DPI. C) Quantification of bacterial burden at 5 DPI after overnight drug treatment initiated at 4 DPI. D) Quantification of bacterial burden in embryos infected with *M.marinum*-tdTomato, injected with clodronate liposomes and treated with tirofiban from at 3 DPI. E) Representative images of bacterial granulomas chosen for analysis (bacteria are white in greyscale images), and corresponding Oil Red O (ORO) staining (red-brown in color images). F) Quantification of ORO pixel density relative to granuloma bacterial area, in embryos treated with tirofiban, normalised to DMSO control. G) Representative images of bacterial granulomas showing bacteria in red and TUNEL staining in green. F) Quantification of TUNEL positive area within the largest granuloma of individual embryos.

All graphs show Mean ± SEM, statistical tests by T-tests. Data are combined results of two independent experiments, except D) and H) which represent single experiments.

Graphical abstract.

M. marinum indicues two independent haemostatic processes in the zebrafish: ESX1 dependent coagulation (1), and ESX1 independent thrombocyte recruitment (2). Bacteria then induce ESX1 dependent thrombocyte activation - either directly or via the macrophage - (3), which leads to foam cell formation and macrophage necrosis, promoting bacterial growth (4). Inhibition of thrombocyte activation with anti-platelet drugs like Tirofiban, stops this

progression and thereby limits the growth of bacteria. Drugs which reduce coagulation (1) have no effect on bacterial growth.

Supplementary Figure Legends

Figure S1

Related to Figure 1. Quantification of clot formation in warfarin-treated embryos infected with *M. marinum.* Error lines represent mean ± SEM, statistical analysis by T test.

Figure S2

Related to Figure 1. A) Representative images of 5 DPI *Tg(cd41:GFP)* embryos infected with *M.marinum*-tdTomato, showing thrombocyte accumulation (green) at sites of bacterial infection (red). B) Quantification of total thrombocyte *Tg*(*cd41:GFP)* area within the tail of uninfected or WT *M.marinum*-tdTomato infected embryos. C) Correlation between *M. marinum* bacterial burden and total thrombocyte *Tg*(*cd41:GFP)* area within the tail of infected embryos. D) Quantification of total thrombocyte *Tg*(*cd41:GFP)* area within the tail of uninfected or ΔESX1 *M.marinum*-tdTomato infected larvae at 5 DPI. E) Correlation between ΔESX1 *M. marinum* bacterial burden and total thrombocyte *Tg* (*cd41:GFP)* area within the tail of infected embryos at 5 DPI.

Figure S3

Related to Figure 1. Images of 2 DPI, 3 DPI and 4 DPI *Tg(cd41:GFP)* embryos infected with *M.marinum*-tdTomato at 3 DPF. At each time-point, 2 images were taken ~10 seconds apart. Thrombocytes located in the same position in both images were considered stationary (non-circulating), and labelled with a white arrow head.

Graphs show Mean ± SEM, statistical testing by T-test or linear regression.

Figure S4

Related to Figure 2. A) Representative images of thrombocyte accumulation at tail wound in 4 DPF *Tg(cd41:GFP)* embryos , 4 hours post injury (hpi). B) Quantification of thrombocytes within 100 μm of the cut site 4 hpi in aspirin-treated embryos. C) Quantification of thrombocytes within 100 μm of the cut site 4 hpi in tirofiban-treated embryos.

Graphs show Mean ± SEM, statistical testing by T-test (B and C) or ANOVA (D).

Figure S5

Related to Figure 3. A) Quantification of thrombocytes within 100 μm of the cut site 4 hours after injury in *itga2b* WT, heterozygous and knock-out embryos. B) Representative images of *Tg(cd41:gfp) itga2b* mutant embryos infected with *M. marinum*-tdTomato. C) Quantification of total thrombocyte *Tg*(*cd41:GFP)* area within the tail of infected *itga2b* mutant embryos.

Figure S6

Related to Figure 4. A) Quantification of bacterial burden in embryos infected with a low dose of 10-50 fluorescent *M. marinum* and treated with tirofiban. **B)** Representative images of caudal haematopoietic tissue in 6 DPF *Tg(mfap4:tdTomato)* embryos, where macrophages are fluorescently labelled, injected with clodronate or PBS liposomes at 4 DPF. **C)** Quantification of macrophage number by fluorescent pixel count at 5 DPI in embryos injected with clodronate or PBS liposomes at 3 DPI, and treated with tirofiban. Graphs show Mean ± SEM, statistical tests by T-tests (A and B) or ANOVA (D).

Methods

Zebrafish husbandry

Adult zebrafish were housed at the Garvan Institute of Medical Research Biological Testing Facility (St Vincent's Hospital AWC Approval 1511) and embryos were produced by natural spawning for infection experiments at the Centenary Institute (Sydney Local Health District AWC Approval 2016-022). Zebrafish embryos were obtained by natural spawning and embryos were raised at 28°C in E3 media.

Zebrafish lines

Wild type zebrafish are the TAB background. Transgenic lines are: *Tg(fabp10a:fgb-EGFP)*^{mi4001} referred to as *Tg(fabp10a:fgb-EGFP)(Vo et al., 2013)*, *Tg(-6.0itga2b:eGFP)*^{la2} referred to as *Tg(cd41:EGFP)(Lin et al., 2005)*, *Tg(mfap4:tdTomato)*^{xt12} referred to as *Tg(mfap4:tdTomato)(Walton et al., 2015)*, Mutant allele *fga*^{mi} contains a 26 bp insertion in the *fibrinogen alpha chain* gene (manuscript in preparation).

Infection of zebrafish embryos

Aliquots of single cell suspensions of midlog-phase *Mycobacterium marinum* M strain, ΔESX1 *M. marinum* and *Pseudomonas aeruginosa* PA01 were frozen at -80°C for use in infection experiments. Bacterial aliquots were thawed and diluted with phenol red dye (0.5% w/v). 10-15 nL was injected into the caudal vein or trunk of M-222 (tricaine)-anaesthetised 30-48 hpf embryos resulting in a standard infectious dose ~400 fluorescent *M. marinum*. Embryos were recovered into E3 supplemented with 0.036 g/L PTU, housed at 28 °C and imaged on day 5 of infection unless otherwise stated.

Drug treatments

Embryos were treated with vehicle control (DMSO or water as appropriate), 10 µg/ml aspirin, 20 µg/ml tirofiban, 10 µM eptifibatide, or 5 µM warfarin. Drugs and E3 were replaced on days 0, 2, and 4 days post infection (DPI) unless otherwise stated.

Tail wound thrombosis assay

3 day post fertilisation (DPF) embryos were treated over-night with anti-platelet drugs. They were anaesthetised, and then a small amount of their tail was removed with a scalpel. Embryos were imaged 4 hours post wounding and the number of GFP positive cells within 100 µm of the cut site was counted.

Imaging

Live zebrafish embryos were anaesthetized in M-222 (Tricaine) and mounted in 3% methylcellulose for imaging on a Leica M205FA or DM6000B fluorescence stereomicroscope. Image analysis was carried out with Image J Software Version 1.51j using fluorescent pixel counts and intensity measurements as previously described (Matty et al., 2016).

Axenic culture

A midlog culture of fluorescent *M. marinum* was diluted 1:100 and aliquoted into 96 well plates for drug treatment. Cultures were maintained at 28°C in a static incubator and bacterial fluorescence was measured in a plate reader.

Morpholinos:

Embryos were injected at the single cell stage with 1 pmol cMPL (5′-CAGAACTCTCACCCTTCAATTATAT-3′), or control morpholino (5′-CCTCTTACCTCAGTTACAATTTATA-3′).

Clodronate liposome injections:

Larvae were injected at 3 DPI (4 DPF) with 10 nl of 5 mg/ml clodronate liposomes or 5 mg/ml PBS vehicle liposomes by caudal vein injection.

Oil-red O:

Oil Red O lipid staining on whole mount embryos was performed and analysed as previously described (Johansen et al., 2018; Passeri et al., 2009). Briefly, embryos were individually imaged for bacterial distribution by fluorescent microscopy, fixed, and stained in Oil Red O (0.5% w/v in propylene glycol). Oil Red O density was calculated by using the ‘measure’ function in Image J, and subtracting the mean brightness of a representative region within each granuloma from the mean brightness of a representative adjacent ‘background’ region.

Statistics

All t-tests were unpaired t-tests with Welch’s correction. All ANOVA were ordinary one-way ANOVA, comparing the mean of each group with the mean of every other group, using Turkey’s multiple comparisons test with a single pooled variance. In cases where data was pooled from multiple experiments, data from each was normalised to its own within-experiment control (usually ‘DMSO’) before pooling. Outliers were removed using ROUT, with Q=1%.

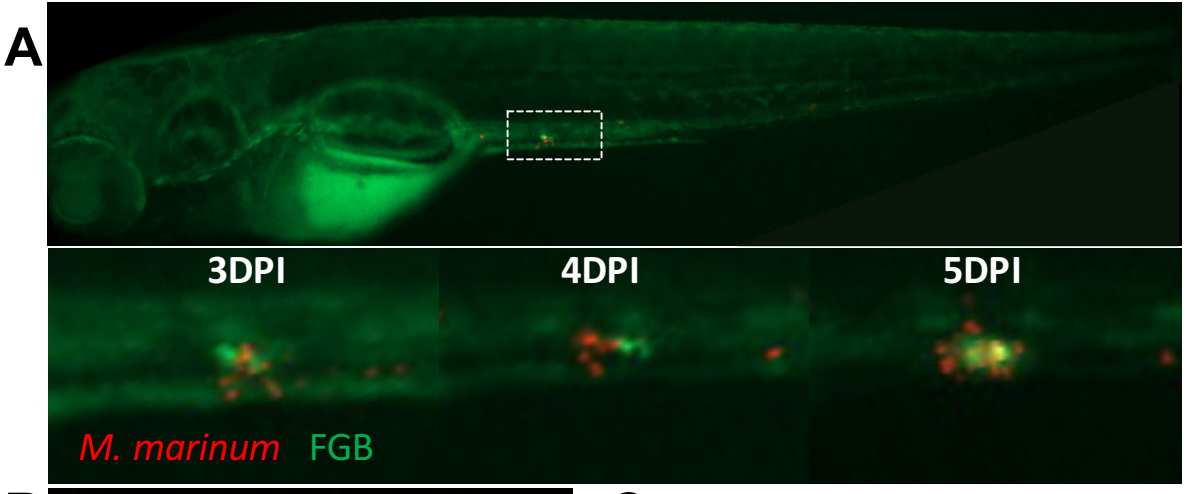
A
3DPI
4DPI
5DPI
M. marinum FGB

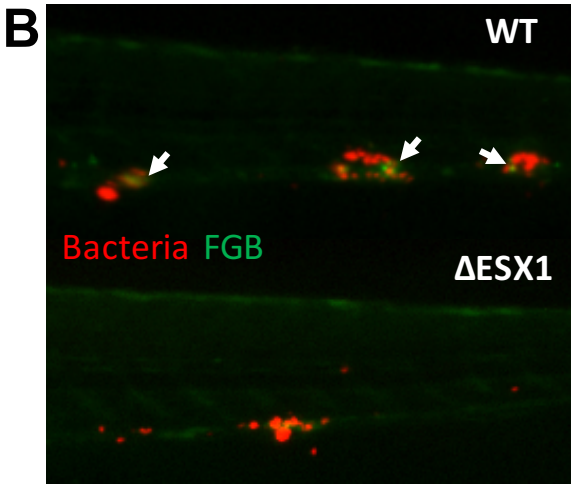
B
WT
Bacteria FGB
ΔESX1

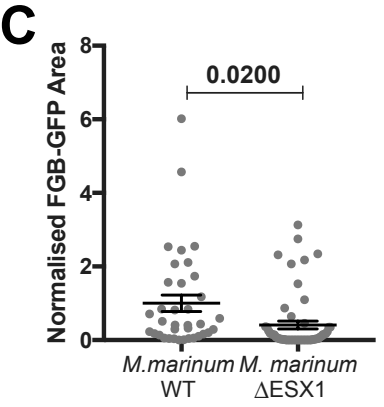
C
Normalised FGB-GFP Area
0.0200
M.marinum WT
M. marinum ΔESX1

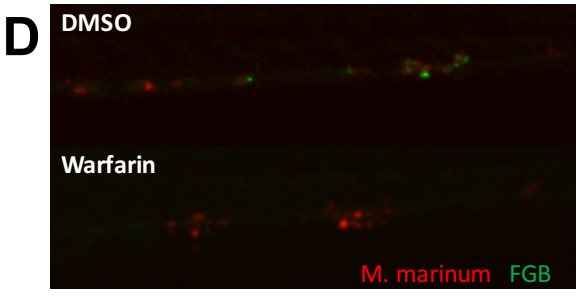
D
DMSO
Warfarin
M. marinum FGB

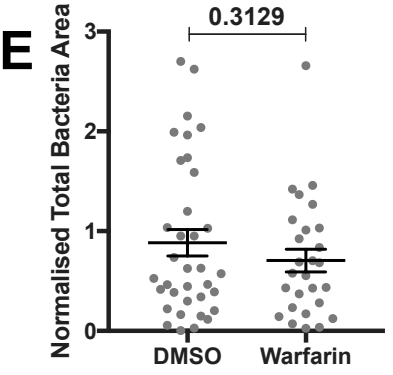
E
Normalised Total Bacteria Area
0.3129
DMSO
Warfarin

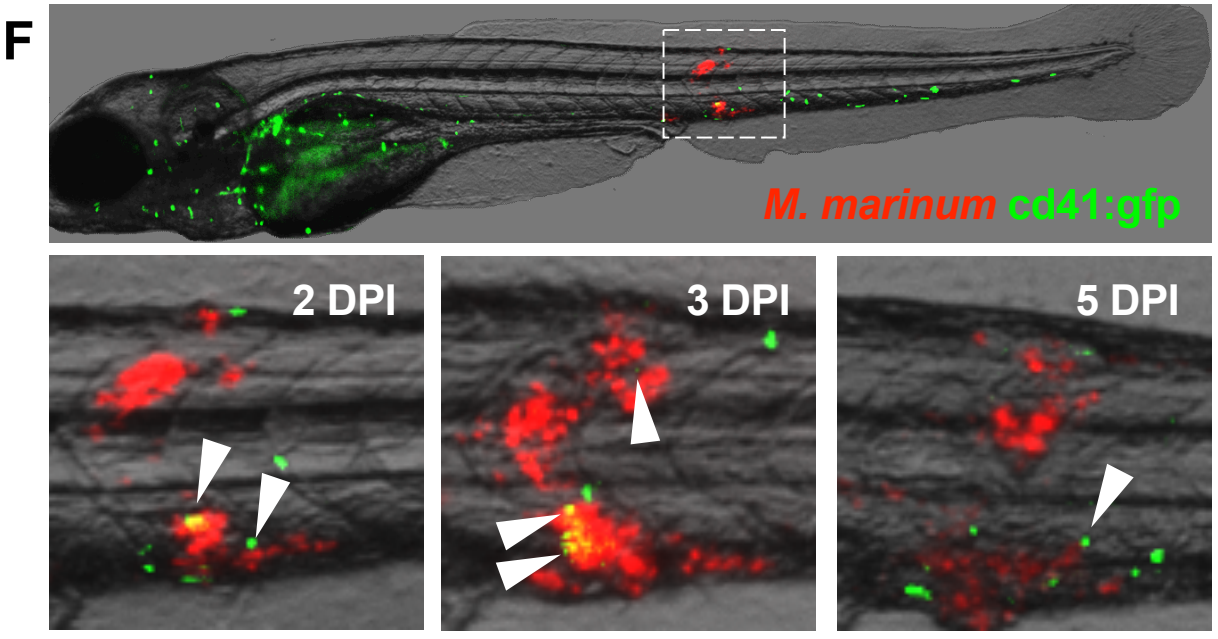
F
M. marinum cd41:gfp
2 DPI
3 DPI
5 DPI

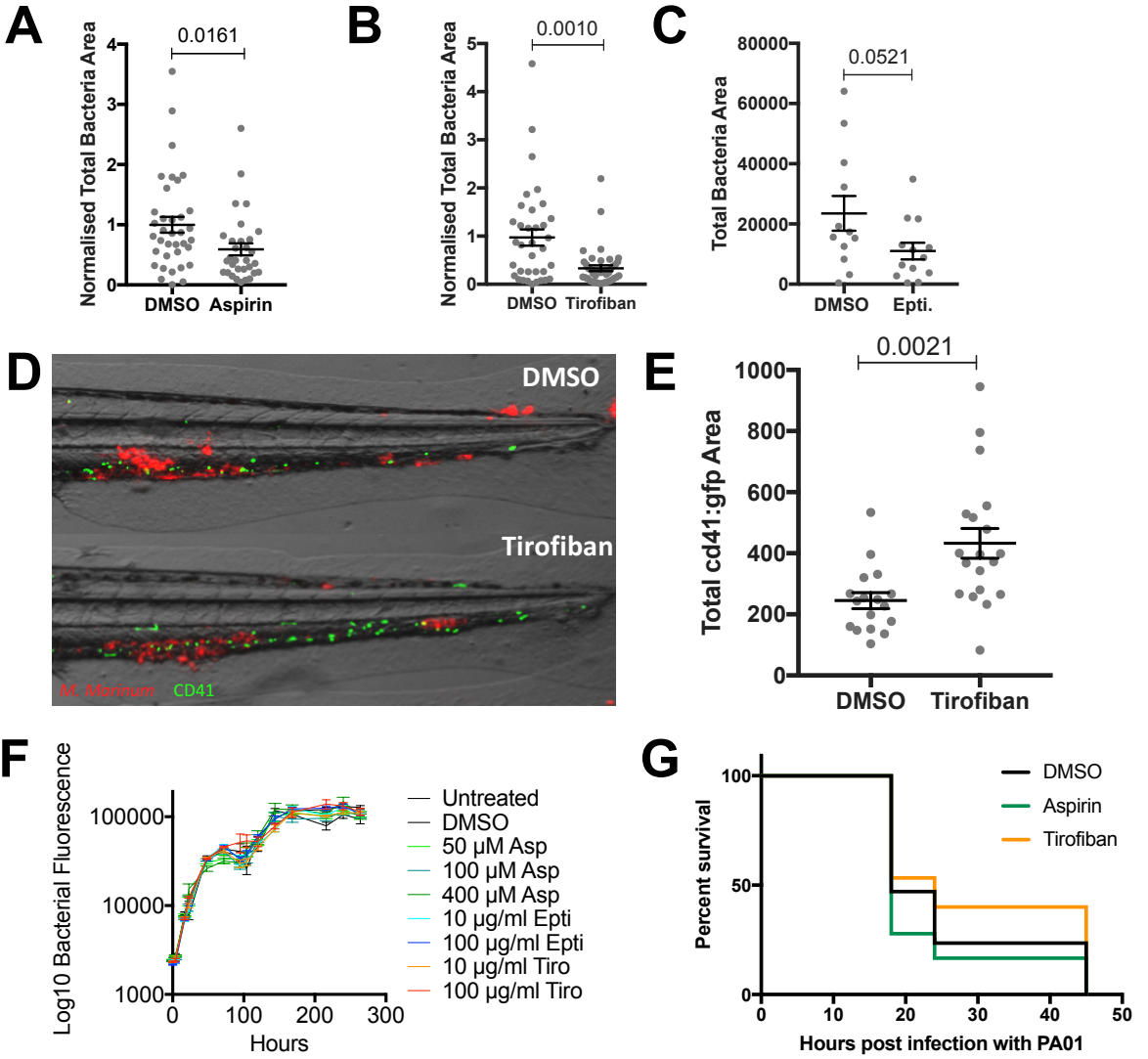
A
0.0161
Normalised Total Bacteria Area
DMSO
Aspirin
B
0.0010
Normalised Total Bacteria Area
DMSO
Tirofiban
C
0.0521
Total Bacteria Area
DMSO
Epti.
D
DMSO
Tirofiban
M. Marinum
CD41
E
0.0021
Total cd41:gfp Area
DMSO
Tirofiban
F
Log10 Bacterial Fluorescence
Hours
Untreated
DMSO
50 µM Asp
100 µM Asp
400 µM Asp
10 µg/ml Epti
100 µg/ml Epti
10 µg/ml Tiro
100 µg/ml Tiro
G
Percent survival
Hours post infection with PA01
DMSO
Aspirin
Tirofiban

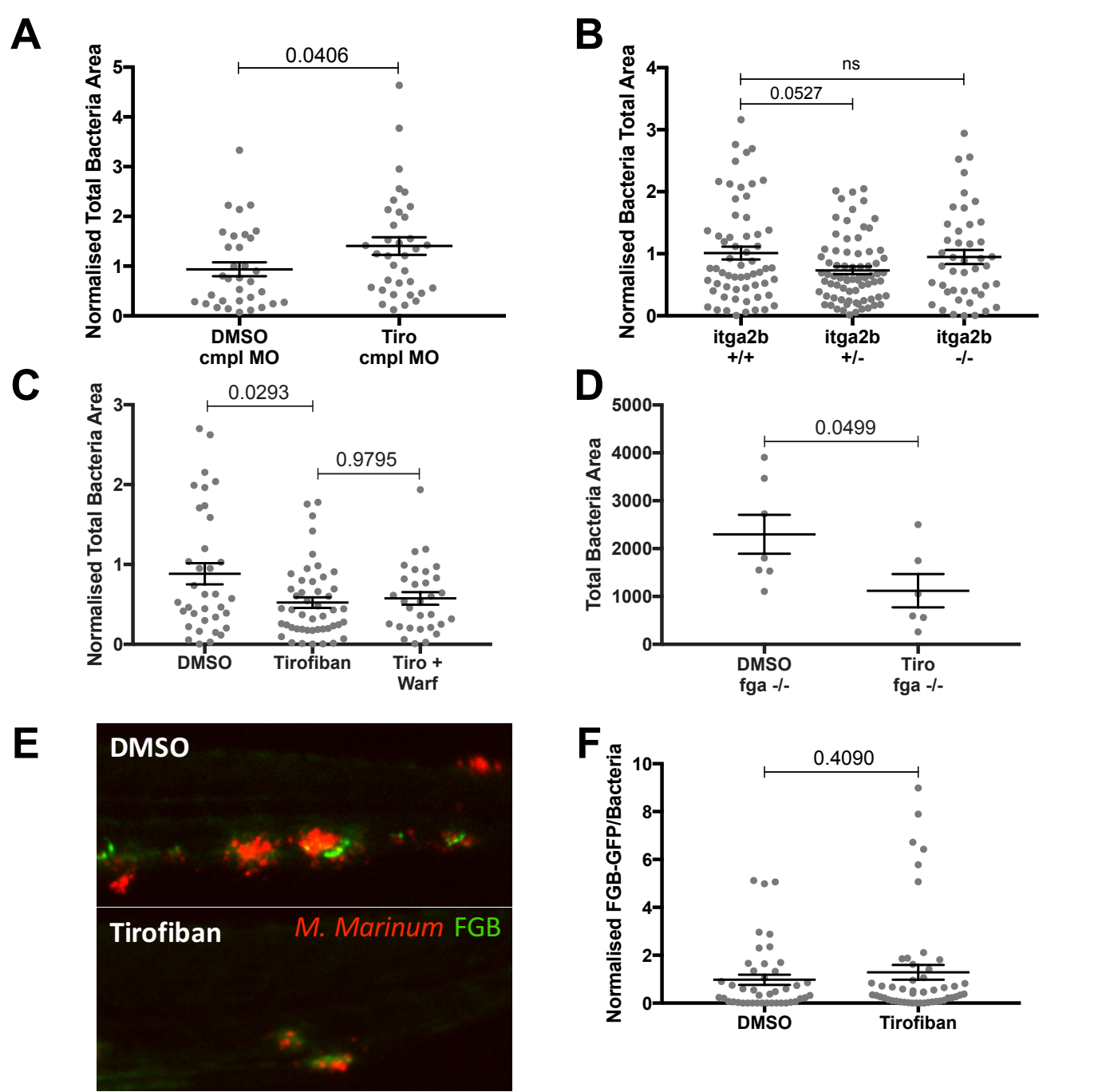
A
Normalised Total Bacteria Area
0.0406
DMSO cmpl MO
Tiro cmpl MO
B
Normalised Bacteria Total Area
ns
0.0527
itga2b +/+
itga2b +/-
itga2b -/-
C
Normalised Total Bacteria Area
0.0293
0.9795
DMSO
Tirofiban
Tiro + Warf
D
Total Bacteria Area
0.0499
DMSO fga -/-
Tiro fga -/-
E
DMSO
Tirofiban
M. Marinum FGB
F
Normalised FGB-GFP/Bacteria
0.4090
DMSO
Tirofiban

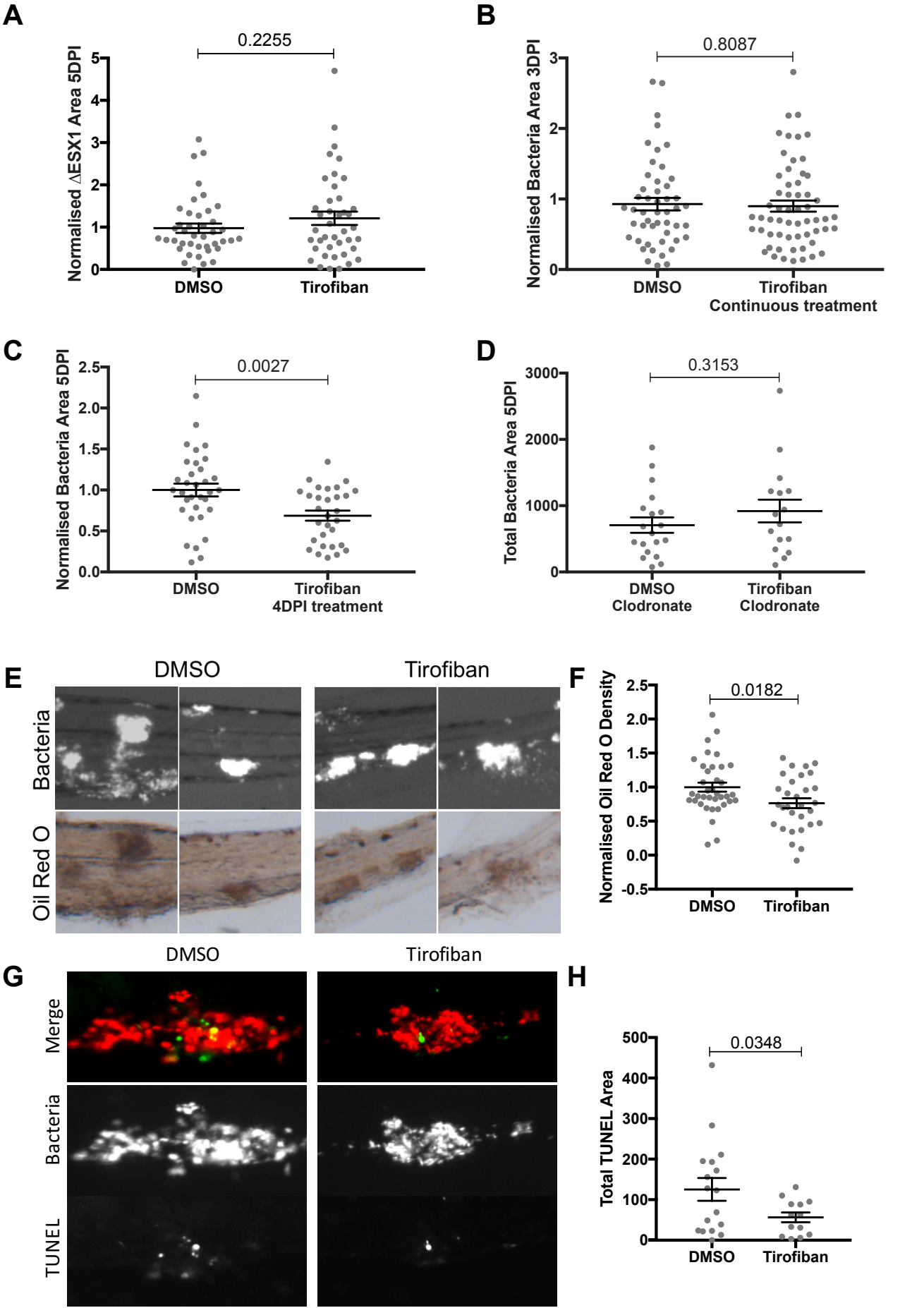
A
0.2255
Normalised ΔESX1 Area 5DPI
DMSO
Tirofiban
B
0.8087
Normalised Bacteria Area 3DPI
DMSO
Tirofiban
Continuous treatment
C
0.0027
Normalised Bacteria Area 5DPI
DMSO
Tirofiban
4DPI treatment
D
0.3153
Total Bacteria Area 5DPI
DMSO
Clodronate
Tirofiban
Clodronate
E
DMSO
Tirofiban
Bacteria
Oil Red O
F
0.0182
Normalised Oil Red O Density
DMSO
Tirofiban
G
DMSO
Tirofiban
Merge
Bacteria
TUNEL
H
0.0348
Total TUNEL Area
DMSO
Tirofiban

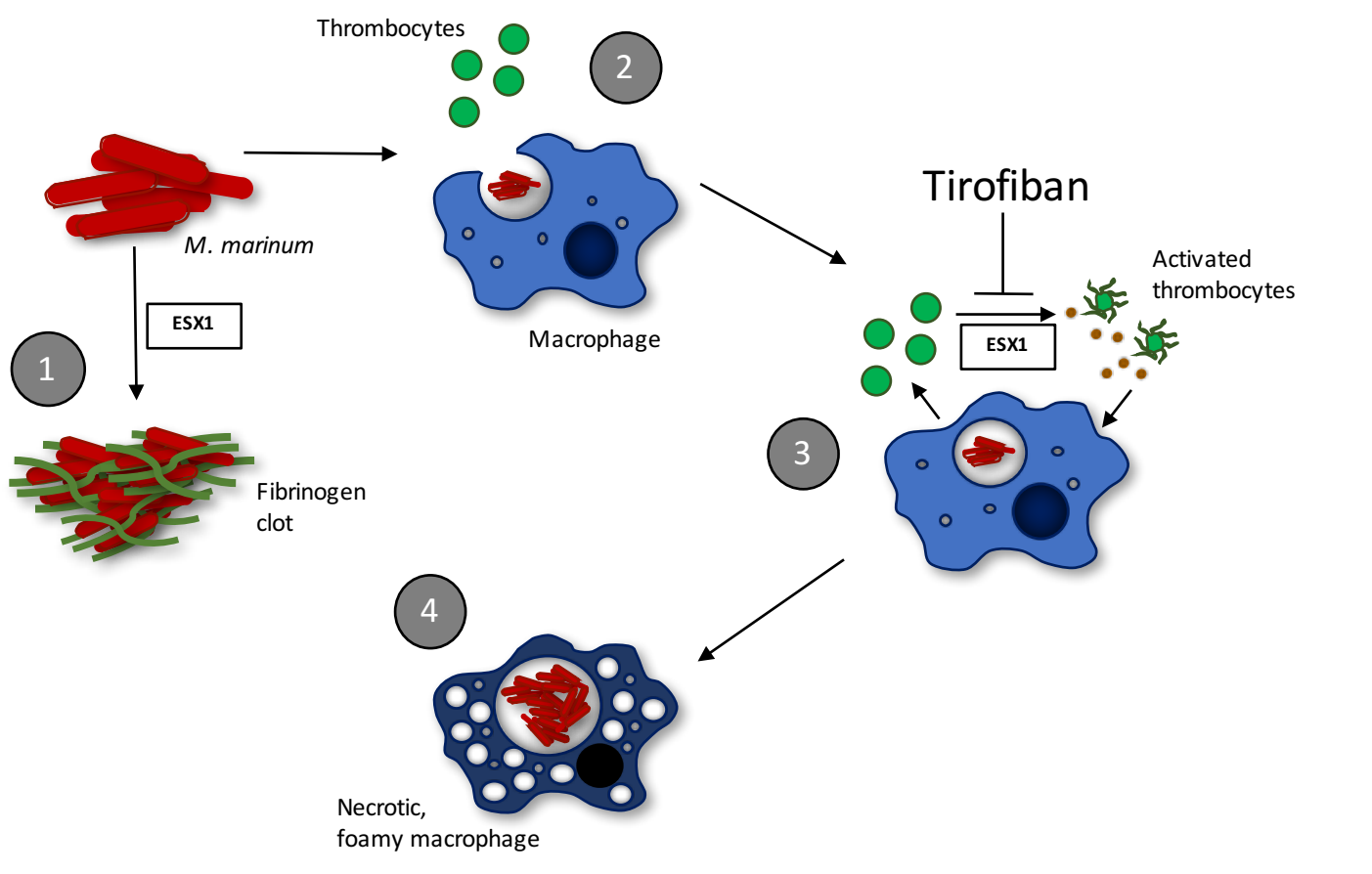
Thrombocytes
2
M. marinum
ESX1
1
Fibrinogen
clot
Macrophage
Tirofiban
Activated
thrombocytes
ESX1
3
4
Necrotic,
foamy macrophage

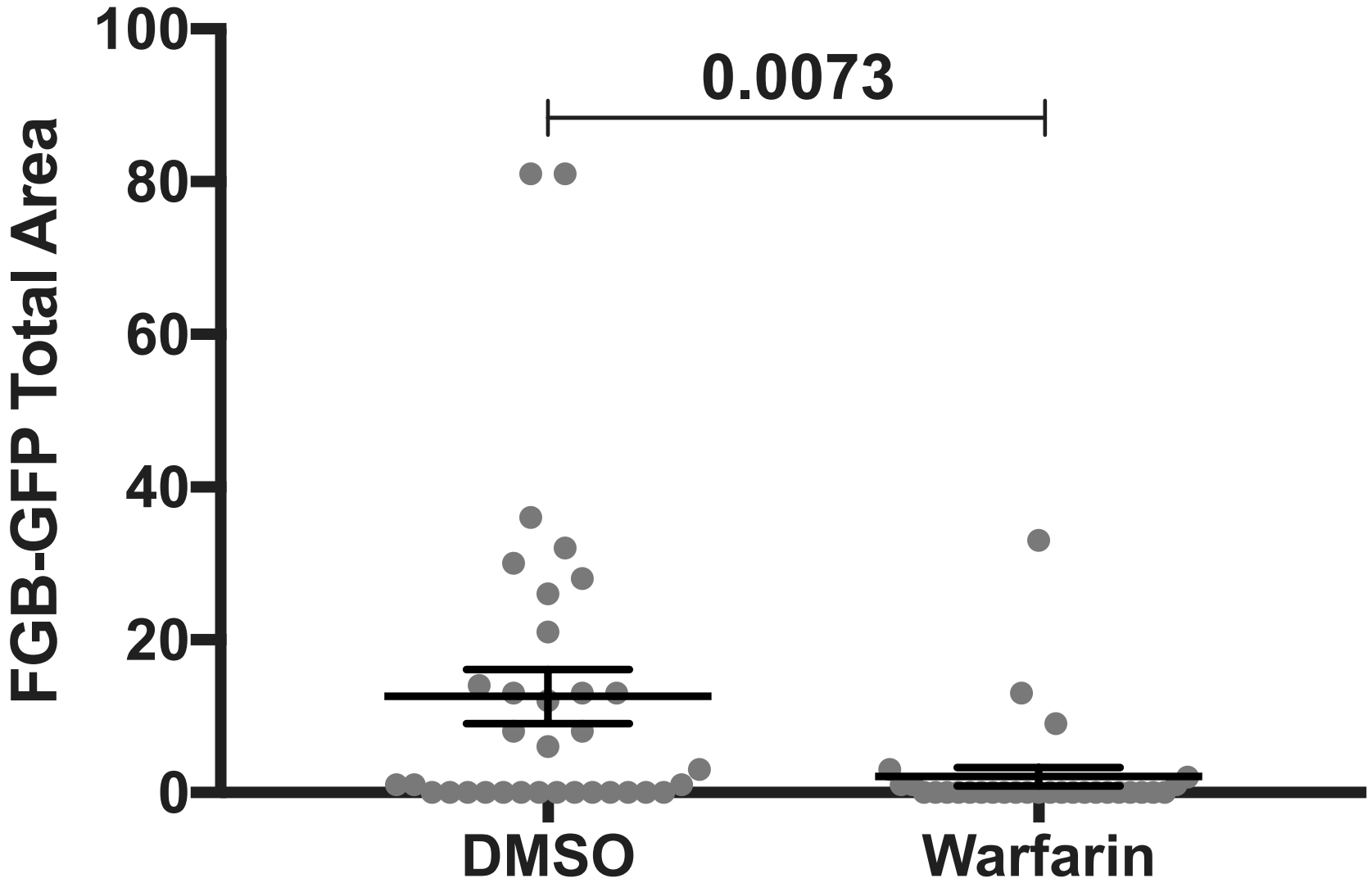
0.0073
FGB-GFP Total Area
100
80
60
40
20
0
DMSO
Warfarin

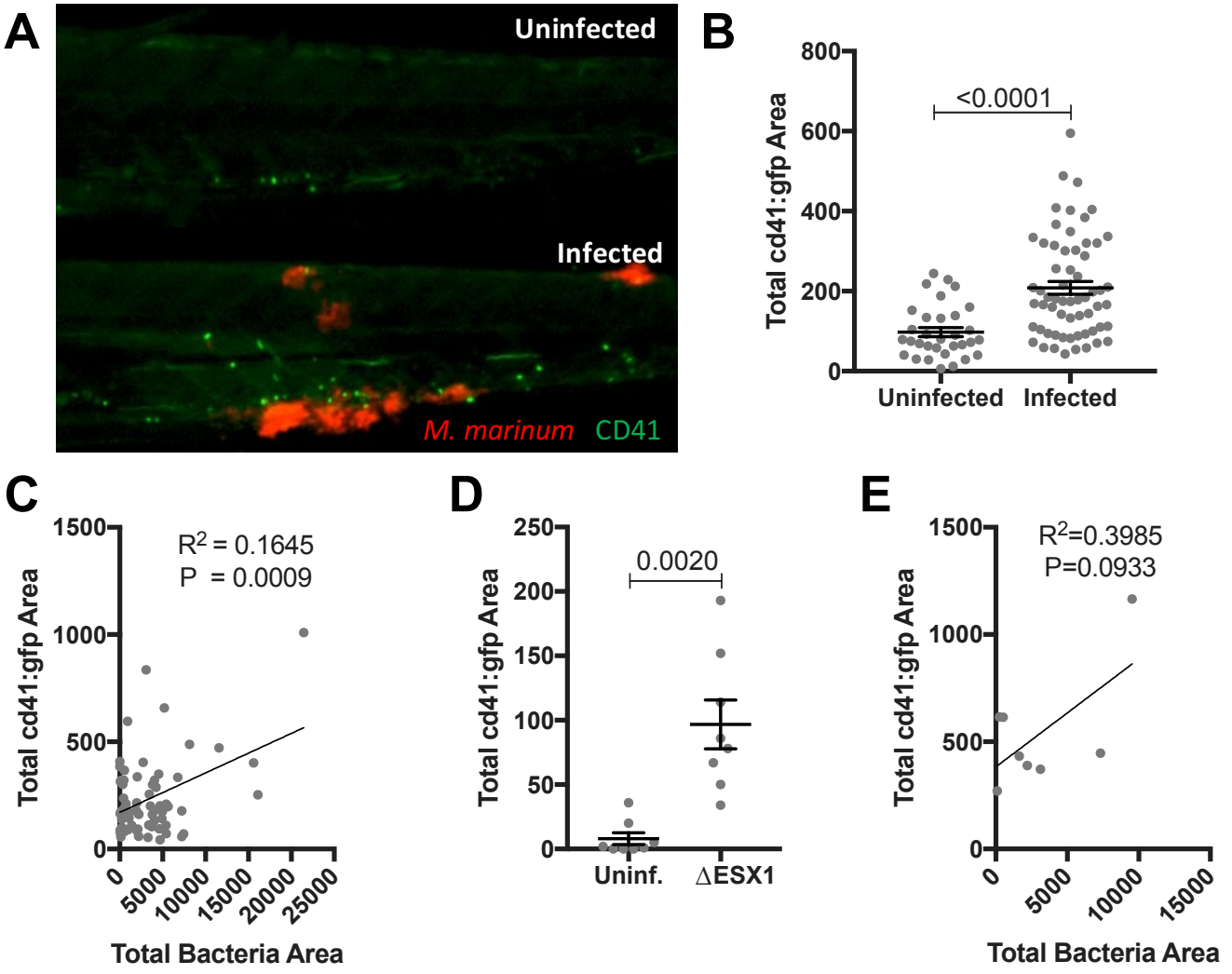
A
Uninfected
Infected
M. marinum
CD41
B
Total cd41:gfp Area
800
600
400
200
0
<0.0001
Uninfected
Infected
C
Total cd41:gfp Area
1500
1000
500
0
R2 = 0.1645
P = 0.0009
0
5000
10000
15000
20000
25000
Total Bacteria Area
D
Total cd41:gfp Area
250
200
150
100
50
0
0.0020
Uninf.
ΔESX1
E
Total cd41:gfp Area
1500
1000
500
0
R2=0.3985
P=0.0933
0
5000
10000
15000
Total Bacteria Area

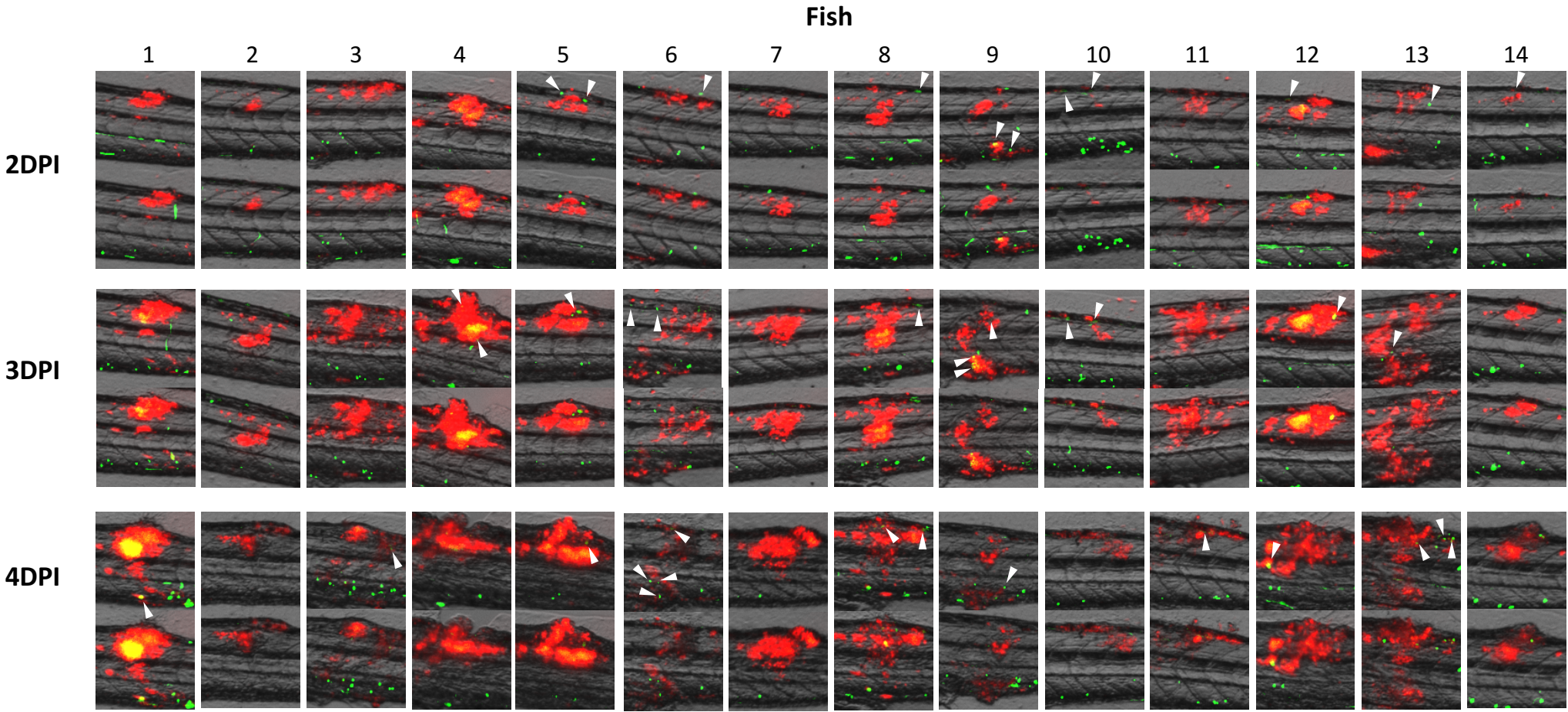
Fish
1
2
3
4
5
6
7
8
9
10
11
12
13
14
2DPI
3DPI
4DPI

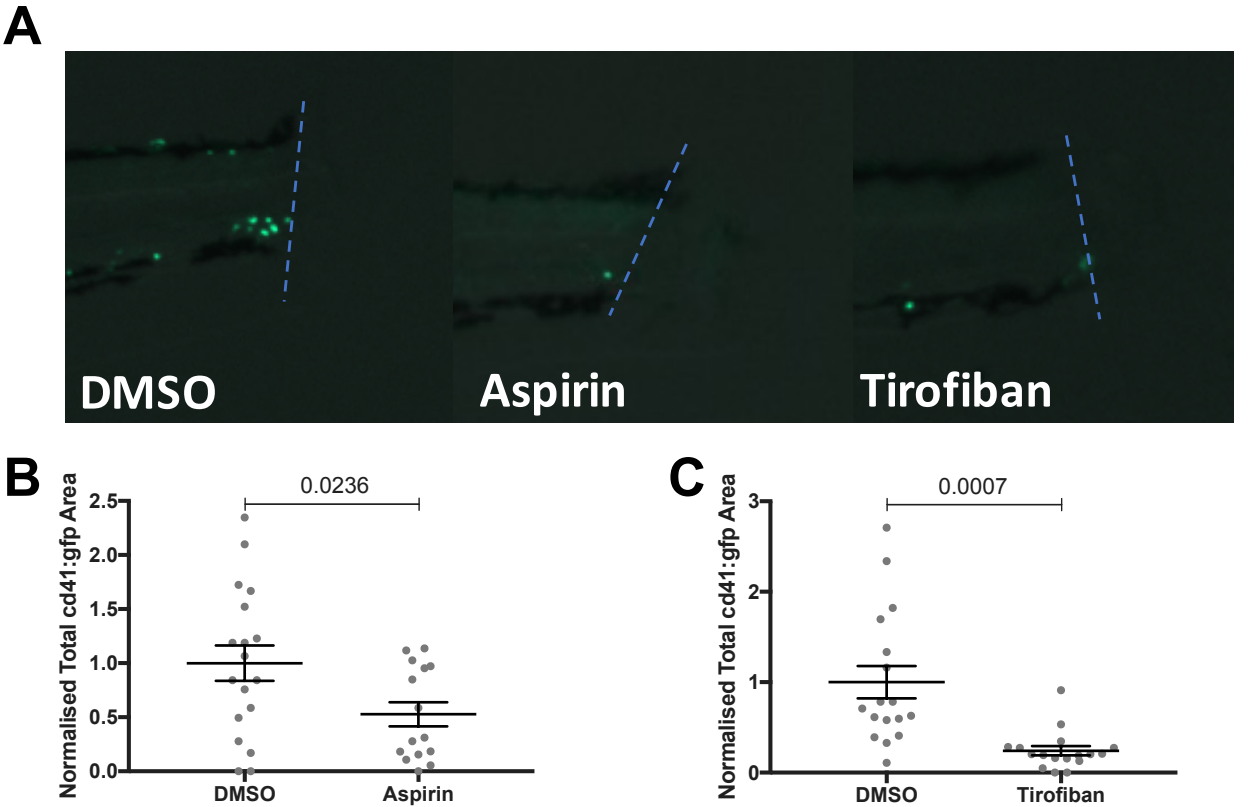
A
DMSO
Aspirin
Tirofiban
B
0.0236
Normalised Total cd41:gfp Area
2.5
2.0
1.5
1.0
0.5
0.0
DMSO
Aspirin
C
0.0007
Normalised Total cd41:gfp Area
3
2
1
0
DMSO
Tirofiban

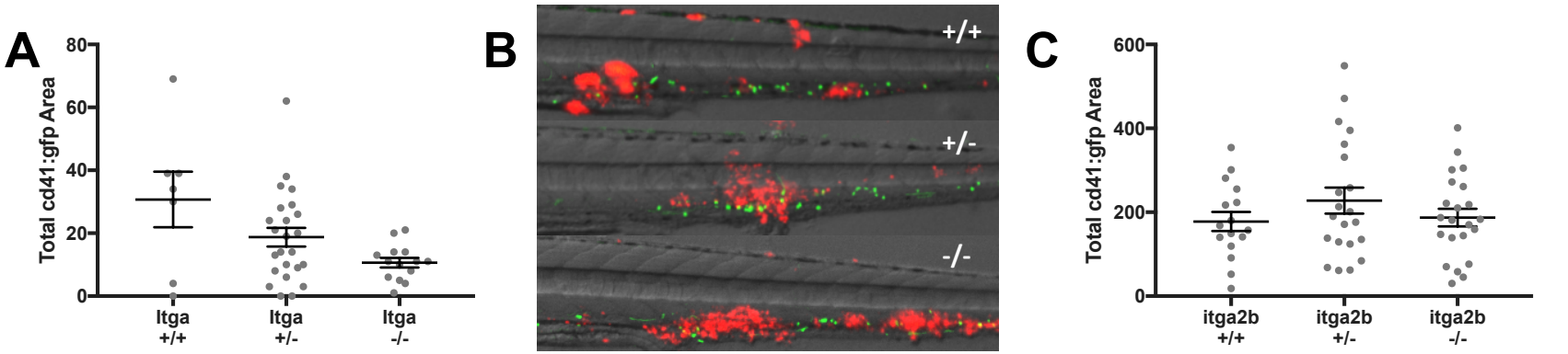
A
Total cd41:gfp Area
80
60
40
20
0
Itga +/+
Itga +/-
Itga -/-
B
+/+
+/-
-/-
C
Total cd41:gfp Area
600
400
200
0
itga2b +/+
itga2b +/-
itga2b -/-

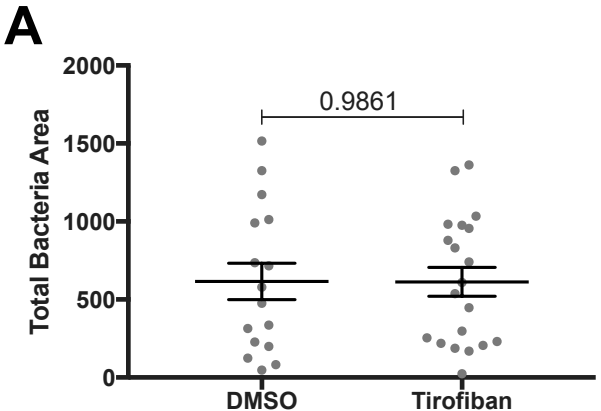
A
Total Bacteria Area
2000
1500
1000
500
0
0.9861
DMSO
Tirofiban

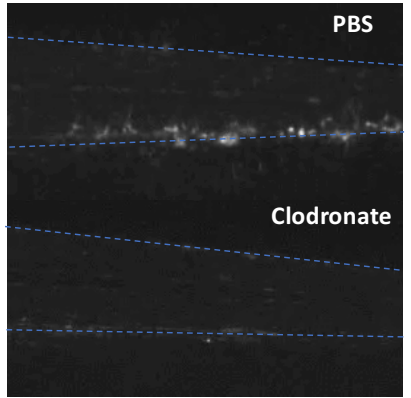
B
PBS
Clodronate

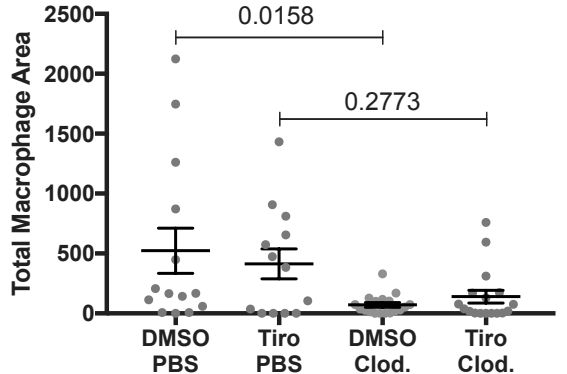
C
Total Macrophage Area
2500
2000
1500
1000
500
0
0.0158
0.2773
DMSO PBS
Tiro PBS
DMSO Clod.
Tiro Clod.